

# Effect of geometric and electronic structures on the finite temperature behavior of $\text{Na}_{58}$ , $\text{Na}_{57}$ , and $\text{Na}_{55}$ clusters

Mal-Soon Lee\* and D. G. Kanhere†

Centre for Modeling and Simulation, and Department of Physics,  
University of Pune, Ganeshkhind, Pune 411 007, India.

(Dated: October 7, 2018)

An analysis of the evolutionary trends in the ground state geometries of  $\text{Na}_{55}$  to  $\text{Na}_{62}$  reveals  $\text{Na}_{58}$ , an electronic closed-shell system, shows namely an electronically driven spherical shape leading to a disordered but compact structure. This structural change induces a strong *connectivity* of short bonds among the surface atoms as well as between core and surface atoms with inhomogeneous strength in the ground state geometry, which affects its finite-temperature behavior. By employing *ab initio* density-functional molecular dynamics, we show that this leads to two distinct features in specific heat curve compared to that of  $\text{Na}_{55}$ : (1) The peak is shifted by about 100 K higher in temperature. (2) The transition region becomes much broader than  $\text{Na}_{55}$ . The inhomogeneous distribution of bond strengths results in a broad melting transition and the strongly connected network of short bonds leads to the highest melting temperature of 375 K reported among the sodium clusters.  $\text{Na}_{57}$ , which has one electron less than  $\text{Na}_{58}$ , also possesses stronger short-bond network compared with  $\text{Na}_{55}$ , resulting in higher melting temperature (350 K) than observed in  $\text{Na}_{55}$ . Thus, we conclude that when a cluster has nearly closed shell structure not only geometrically but also electronically, it shows a high melting temperature. Our calculations clearly bring out the size-sensitive nature of the specific heat curve in sodium clusters.

PACS numbers: 31.15.Ew, 36.40.Cg, 36.40.Ei, 64.70.Dv, 71.15.Mb

## I. INTRODUCTION

The finite-temperature behavior of sodium clusters has been attracted much attention since the pioneering experimental work by Haberland and co-workers.<sup>1,2</sup> These experiments reported melting temperatures of sodium clusters in the size range of 55 to 350 atoms. A great deal of effort has been spent to understand and explain the main puzzling feature, namely the irregular variation in the observed melting points. Equally puzzling is the observation that  $\text{Na}_{57}$  and  $\text{Na}_{142}$ , which is neither geometric shell-closing systems nor electronic shell-closing systems, show higher melting temperatures than vicinity systems such as  $\text{Na}_{55}$  and  $\text{Na}_{147}$  of geometric shell-closing ones or  $\text{Na}_{138}$  of electronic shell-closing one, which is not explained so far. Although it is expected that there is an intricate interplay between the electronic and geometric structures so far as finite temperature behavior is concerned, the consensus seems to be that the geometry dominates the melting characteristics and the effects of electronic structure are secondary.<sup>2,3</sup> This has been a surprise since the stability of these clusters is almost entirely dictated by the electronic structure. **According to our present calculations, it reveals that when a cluster with nearly electronic closed shell structure has nearly icosahedral ground state geometry, it shows a high melting temperature.**

Recently a very different aspect of the finite-temperature behavior has been revealed in the experimental measurements of heat capacities of gallium and aluminum clusters,<sup>4</sup> namely the size-sensitive nature of their *shapes*. A definitive correlation between the shape of specific heat curve and the nature of the ground-state

geometry in gallium cluster has also been established by our group.<sup>13</sup> Surprisingly, in spite of extensive work reported on the bench mark system of sodium clusters, there is no report of such a size sensitivity.

In this paper, we show the effect of electronic structure on the melting of sodium cluster by comparison to a geometric shell-closing system. It is interesting to note that there are very few cases in sodium clusters where an electronic shell-closing system ( $N=8, 20, 40, 58, 138, \dots$ ) has a similar size as a geometric shell-closing one ( $N=55, 147, 309, \dots$ ). For instance, a pair of clusters  $N=55$  and  $N=58$  differs by three atoms only. Another example is a pair  $\{N=138 \text{ and } 147\}$  having nine-atom difference. The next such occurrence is at  $N=309$  and  $N=338$ , which is not close enough. Therefore, the expected effects due to both the geometric and electronic magic numbers are likely to be seen prominently in  $\{55, 58\}$  range. The electronically closed-shell structure of  $\text{Na}_{58}$  and nearly electronic shell closing system of  $\text{Na}_{57}$  have slightly distorted icosahedral structures as their ground state geometries compared to the geometric shell-closing cluster of  $\text{Na}_{55}$ . Indeed, as we shall see,  $\text{Na}_{58}$  and  $\text{Na}_{57}$ , have significantly different finite-temperature characteristics as compared to those of geometrically closed-shell cluster,  $\text{Na}_{55}$ . Firstly, the shape of the specific heat curve is much broader than that of  $\text{Na}_{55}$ . Secondly, it shows a peak (rather broad) at the temperature approximately 375 K for  $\text{Na}_{58}$  and 350 K for  $\text{Na}_{57}$ . We note that the observed melting temperature of  $\text{Na}_{57}$  by Haberland and co-workers<sup>1</sup> is about 325 K which differs less than 8 % from our result. Specially, in case of  $\text{Na}_{58}$  this is the first observation that a melting temperature of sodium cluster can be closed to that of the bulk. Interestingly, it is

observed that  $\text{Na}_{58}$  shows high abundance in mass spectra, indicating its high stability.<sup>1</sup> The paper is organized as follows: in Sec. II, we briefly mention computational details used. In Sec. III we discuss our results, and summarize the results in Sec. IV.

## II. COMPUTATIONAL DETAILS

We have carried out Born–Oppenheimer molecular-dynamics simulations using ultrasoft pseudopotentials within the local–density approximation (LDA).<sup>6</sup> The reliability of our calculation can be judged from the fact that our earlier calculations based on density–functional theory (DFT) have successfully reproduced the melting temperature of  $\text{Na}_n$  ( $n=55$ , 92, and 142).<sup>7</sup> In order to get an insight into the evolutionary pattern of the geometries, we have obtained equilibrium structures for  $\text{Na}_n$  ( $n=55$  to 62). Our thorough search of the lowest–energy structure is done by obtaining at least 180 distinguishable equilibrium configurations for each of the clusters by using a combination of a basin–hopping algorithm and density–functional methods. With obtained ground–state geometry of  $\text{Na}_{58}$  and  $\text{Na}_{57}$ , we have carried out extensive *ab initio* constant–temperature simulations using a Nose–Hoover thermostat to compare with geometrically closed shell system,  $\text{Na}_{55}$ . These simulations have been carried out at 16 temperatures for  $\text{Na}_{58}$  and at 12 temperatures for  $\text{Na}_{57}$  in the range of  $80\text{K} \leq T \leq 500\text{K}$  for the period of at least 210 ps (240 ps near the melting temperature), total simulation times of 2.7 ns and 3.5 ns, respectively. Our cell size used is  $24 \times 24 \times 24 \text{ \AA}^3$ , with the energy cutoff of 3.6 Ry whose reliability has been examined in our previous work.<sup>7</sup> With obtained ground–state geometry of  $\text{Na}_{58}$  and  $\text{Na}_{57}$ , we have carried out extensive *ab initio* constant–temperature simulations using a Nose–Hoover thermostat to compare with geometrically closed shell system,  $\text{Na}_{55}$ . These simulations have been carried out at 12 temperatures for  $\text{Na}_{57}$  and at 16 temperatures for  $\text{Na}_{58}$  in the range of  $80\text{K} \leq T \leq 500\text{K}$  for the period of at least 210 ps (240 ps near the melting temperature), total simulation times of 2.7 ns and 3.5 ns, respectively. Our cell size used is  $24 \times 24 \times 24 \text{ \AA}^3$ , with the energy cutoff of 3.6 Ry whose reliability has been examined in our previous work.<sup>7</sup> We use the multiple–histogram technique to calculate specific heat. More details of the methods can be found in Ref. 8. For the analysis, we have taken the last 165 ps data from each temperature, leaving at least first 45 ps for thermalization.

## III. RESULTS AND DISCUSSION

The lowest–energy structures of  $\text{Na}_n$  ( $n=55$ –62) are shown in Fig. 1. There are some striking features evident in their evolutionary pattern. The ground–state geometry (GS) of  $\text{Na}_{55}$  is the well–known icosahedron<sup>9</sup>. A single extra atom added to  $\text{Na}_{55}$  is accommodated on the

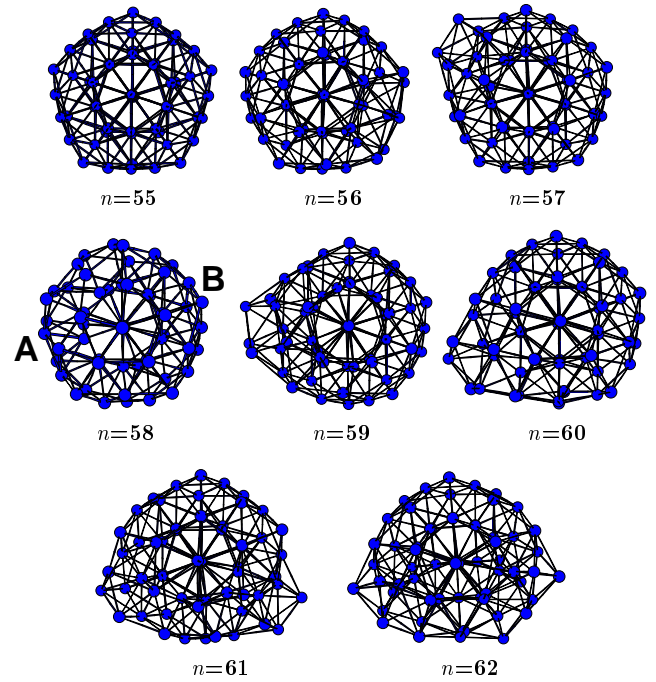


FIG. 1: The ground–state geometry of  $\text{Na}_n$  ( $n=55$ –62). In the figure of  $\text{Na}_{58}$ , “A” indicates the region where three extra atoms are accommodated compared to  $\text{Na}_{55}$ , and “B” indicates the region where the geometry of  $\text{Na}_{55}$  is retained.

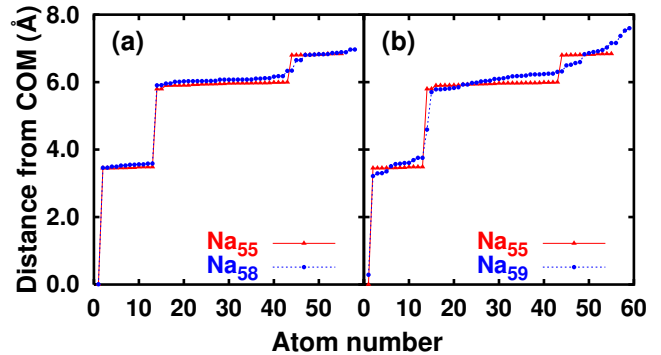


FIG. 2: The distance from the center of mass of  $\text{Na}_{58}$  and  $\text{Na}_{59}$  in comparison with that of  $\text{Na}_{55}$ . In  $\text{Na}_{58}$  the maximum distance is almost the same as seen in  $\text{Na}_{55}$ , while that in  $\text{Na}_{59}$  is changed significantly.

surface by a minor adjustment of surface atoms. When the second atom is added, it is energetically more favorable to retain the icosahedral core with two atoms *capping* it. Very interestingly, when three atoms are added ( $n=58$ ), instead of the pattern of capping continuing, all three atoms are accommodated on the surface of icosahedron, making the structure again nearly spherical without changing the size of  $\text{Na}_{55}$  significantly. This can be verified by examining the distance from the center of mass (COM). In Fig. 2, we show the distance from COM in  $\text{Na}_{58}$  and  $\text{Na}_{59}$  by comparison with those of  $\text{Na}_{55}$ . It is clearly seen that in comparison with the

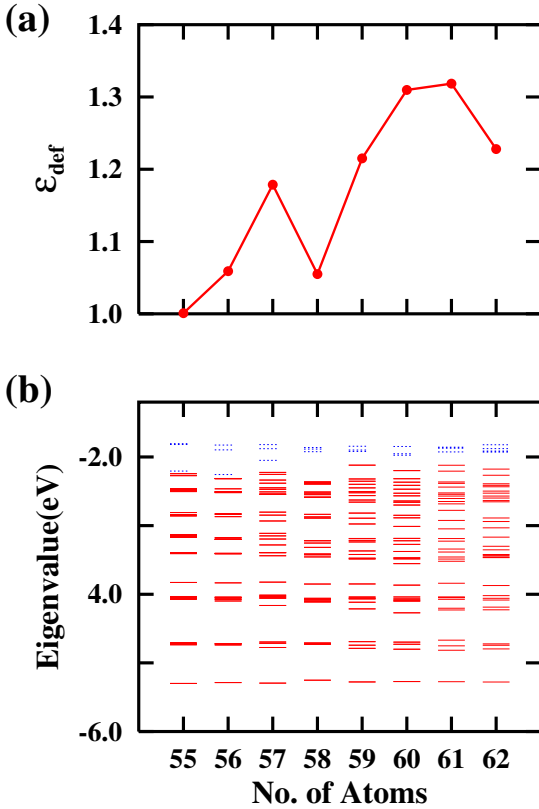


FIG. 3: The comparison of (a) the deformation parameter,  $\varepsilon_{def}$ , (b) the eigenvalue spectra of the ground-state geometries as a function of cluster size.

maximum distance from COM in  $\text{Na}_{55}$ , that in  $\text{Na}_{58}$  is nearly remained the same, while in  $\text{Na}_{59}$  it increases considerably. The pattern of growth from  $\text{Na}_{59}$  to  $\text{Na}_{62}$  changes back to the capping mode as can be seen in Fig. 1. This peculiar shape transformation observed in  $\text{Na}_{58}$  can be examined by plotting deformation parameter  $\varepsilon_{def}$ .  $\varepsilon_{def}$  is defined as  $\varepsilon_{def} = 2Q_1/(Q_2 + Q_3)$ , where  $Q_1 \geq Q_2 \geq Q_3$  are eigenvalues of the quadrupole tensor  $Q_{ij} = \sum_I R_{Ii}R_{Ij}$  with  $R_{Ii}$  being  $i^{th}$  coordinate of ion  $I$  relative to the center of mass of the cluster. For a spherical shape ( $Q_1 = Q_2 = Q_3$ )  $\varepsilon_{def}$  is 1.0, while  $\varepsilon_{def} > 1.0$  indicates a deformation. It can be seen in Fig. 3(a) that the addition of three atoms over  $\text{Na}_{55}$  changes the shape to nearly spherical. Interestingly, this difference is reflected in their eigenvalue spectrum as shown in Fig. 3(b). A peculiarity of  $\text{Na}_{58}$  is that the structure is not highly symmetric, rather in the sense of amorphous. However, it follows jellium-like pattern very closely in contrast to  $\text{Na}_{57}$ ,  $\text{Na}_{59}$  to  $\text{Na}_{62}$  where additional states appear in the gaps due to their disordered structures. Such an effect is absent in  $\text{Na}_{58}$ . In addition an electronic shell-closing system of  $\text{Na}_{58}$  shows the highest gap of the highest occupied molecular orbital (HOMO) and the lowest unoccupied molecular orbital (LUMO) among present studied systems. Thus, an electronically closed-shell nature of  $\text{Na}_{58}$  results into a spherical charge density

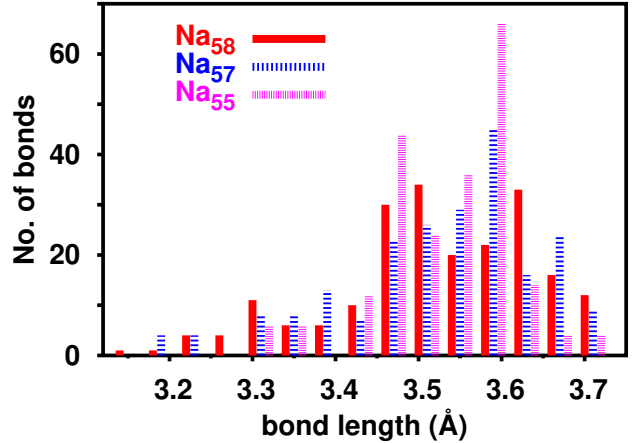


FIG. 4: The histogram of bond lengths for the ground state geometry of  $\text{Na}_{58}$ ,  $\text{Na}_{57}$ , and  $\text{Na}_{55}$ , with less than that of the bulk ( $3.71\text{\AA}$ ).

distribution which drives the geometry towards a spherical shape. Our calculations bring out the fact that this change of shape induces the GS geometry to be compact with a significant structural disorder in  $\text{Na}_{58}$ . This is an example of an *electronically driven shape change*.

We find that to understand the melting behavior of small cluster, which we shall see later, it is important to study not only how many short bonds are there in the GS geometry of the cluster, but also how these short bonds are connected each other (we call this “*connectivity*”). Thus, we have examined the bond lengths in  $\text{Na}_{58}$ ,  $\text{Na}_{57}$ , and  $\text{Na}_{55}$  as well as their connectivity. Fig. 4 shows the number of bonds having bond lengths less than  $3.71\text{\AA}$ , the bulk bond length.  $\text{Na}_{58}$  has 21 bonds shorter than the shortest bond in  $\text{Na}_{55}$ , which are located in the region A, shown in Fig. 1, giving rise to an island of relatively strongly bonded atoms as compared to  $\text{Na}_{55}$ . In  $\text{Na}_{57}$  there are 16 bonds which are shorter than the shortest bond in  $\text{Na}_{55}$ . Fig. 5 shows how the nature of connectivity in these clusters with different bond lengths. In Figs. 5(a)–5(c), connectivity of short bonds are shown with bond lengths less than  $3.45\text{\AA}$ , and Figs. 5(d)–5(f) for less than  $3.55\text{\AA}$ . It can be seen that  $\text{Na}_{55}$  has fewer short bonds (12 bonds) than  $\text{Na}_{58}$  (41 bonds) and  $\text{Na}_{57}$  (38 bonds). The majority of these strong bonded atoms in  $\text{Na}_{58}$  form a connected island in the region A shown in Fig. 1, while all short bonds in  $\text{Na}_{55}$  are radial. It is also evident from Fig. 5(d) that for bond lengths less than  $3.55\text{\AA}$   $\text{Na}_{58}$  shows not only that core atoms are strongly bonded to surface but that even surface atoms are bonded each other. In contrast to this, there is a connectivity only between core (first shell) and surface atoms but not among surface atoms in  $\text{Na}_{55}$  (Fig. 5(f)).  $\text{Na}_{57}$  shows stronger and inhomogeneous connectivity than those seen in  $\text{Na}_{55}$  but weaker than those seen in  $\text{Na}_{58}$  in both bond length regimes. Thus, we conclude that to accommodate three extra atoms in  $\text{Na}_{58}$  first-shell and surface distance is reduced, resulting in a strong network extending over

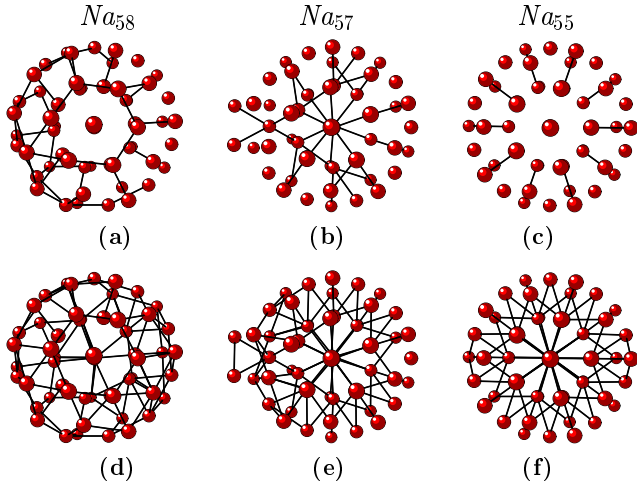


FIG. 5: The short-bond connectivity with bond length less than  $3.45\text{\AA}$  in (a)  $\text{Na}_{58}$  (b)  $\text{Na}_{57}$  (c)  $\text{Na}_{55}$ , showing inhomogeneous distribution of bond strength in  $\text{Na}_{58}$  and  $\text{Na}_{57}$ . The short-bond connectivity with bond length less than  $3.55\text{\AA}$  in (d)  $\text{Na}_{58}$  (e)  $\text{Na}_{57}$  (f)  $\text{Na}_{55}$ , showing  $\text{Na}_{58}$  has strongest connectivity through entire system among three clusters.

entire cluster with inhomogeneous strength. To compare the GS structures of  $\text{Na}_{58}$  and  $\text{Na}_{55}$ , We also analyze the distribution of short bond lengths in  $\text{Na}_{58}$  and  $\text{Na}_{55}$  by comparing the distance from different shells. It turns out that while  $\text{Na}_{55}$  has shorter bond length between center atom and first-shell, the average bond length between first-shell and outer-shell is shorter in  $\text{Na}_{58}$ . In a recent work by Aguado and López,<sup>3</sup> they have attributed the higher melting temperature, seen in experiments of sodium clusters,<sup>1,2</sup> to the existence of shorter bonds between the surface and first-shell atoms. Our calculations are consistent with this observation.

We have examined the electron localization function (ELF). The ELF<sup>10</sup> is defined as

$$\chi_{ELF} = \left[ 1 + \left( \frac{D}{D_h} \right)^2 \right]^{-1}$$

where

$$D = \frac{1}{2} \sum_i |\nabla \psi_i|^2 - \frac{1}{8} \frac{|\nabla \rho|^2}{\rho}$$

$$D_h = \frac{3}{10} (3\pi^2)^{5/3} \rho^{5/3}$$

Here  $\rho \equiv \rho(\mathbf{r})$  is the valence electron density and  $\psi_i$ 's are the KS orbitals. The  $\chi_{ELF}$  is 1.0 for perfect localized function and 0.5 for plain waves. In Fig. 6, we show the ELF isosurface of  $\text{Na}_{58}$  for isovalue of  $\chi_{ELF}=0.79$  in two

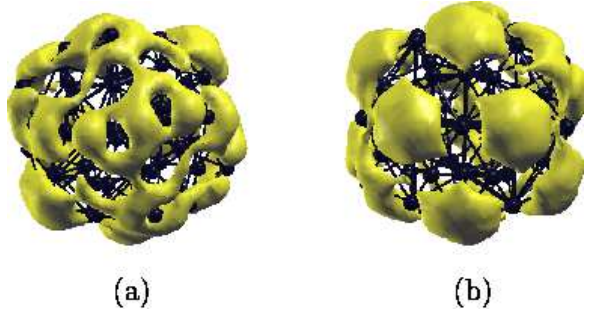


FIG. 6: The isovalued surfaces of the electron localization function at  $\chi_{ELF}=0.79$  for  $\text{Na}_{58}$  (a) in region A and (b) in region B. The similar pattern of (b) is also seen at  $\chi_{ELF}=0.76$  in  $\text{Na}_{55}$ .

different regions. Figs. 6(a) and 6(b) depicts the ELF at 0.79 in regions A and B, respectively. The contrast is evident. In region A which consists of atoms connected by shorter bonds, the ELF isosurface forms a connected network showing the existence of a strongly bonded region containing at least 20 atoms. In contrast, in region B such a network is absent. In fact, the region B gets connected at a lower isovalue of 0.74. The same analysis has been carried out for  $\text{Na}_{57}$  and  $\text{Na}_{55}$ .  $\text{Na}_{57}$  shows similar characteristics compared to those seen in  $\text{Na}_{58}$ . A region near the capping atoms (left-hand side in Fig. 5(b)) starts connecting at  $\chi_{ELF}=0.78$ , whereas a region away from them is connected at 0.74. The connection of isosurface is established over the entire cluster of  $\text{Na}_{55}$  at the isovalue of 0.72. Thus, our ELF analysis clearly brings out the existence of strongly bonded island of atoms and the inhomogeneous distribution of bond strength in  $\text{Na}_{58}$  and  $\text{Na}_{57}$ .

Our study reveals two unique features in the ground state geometries of  $\text{Na}_{58}$  and  $\text{Na}_{57}$ . Firstly, the (nearly) electronic shell closing system induces shortening of bonds, resulting in a strong connectivity of short bonds among the surface atoms as well as between first-shell and surface atoms compared to only first-shell to core connectivity established in  $\text{Na}_{55}$ . Secondly, its ground-state geometry is considerably disordered, resulting in inhomogeneous distribution of bond strength as compared to highly symmetric  $\text{Na}_{55}$ . Here, disordering in these cases is related to the absence of spherical symmetry. We argue that these two effects will be manifested in the specific heat differently. The existence of the well-connected short-bonds are expected to raise the melting temperature as compared to that of  $\text{Na}_{55}$ . The effect of geometric disorder is to broaden the specific heat.

We show the calculated specific-heat curves for  $\text{Na}_{58}$  and  $\text{Na}_{57}$  along with those of  $\text{Na}_{55}$ ,<sup>7</sup> in Fig. 7. The most symmetric cluster  $\text{Na}_{55}$  shows a sharp melting transition at 280 K, while the highest melting temperature is seen in  $\text{Na}_{58}$ . Thus, the addition of two or three atoms changes the specific heat curve drastically. Our calculations clearly demonstrate a strong correlation between

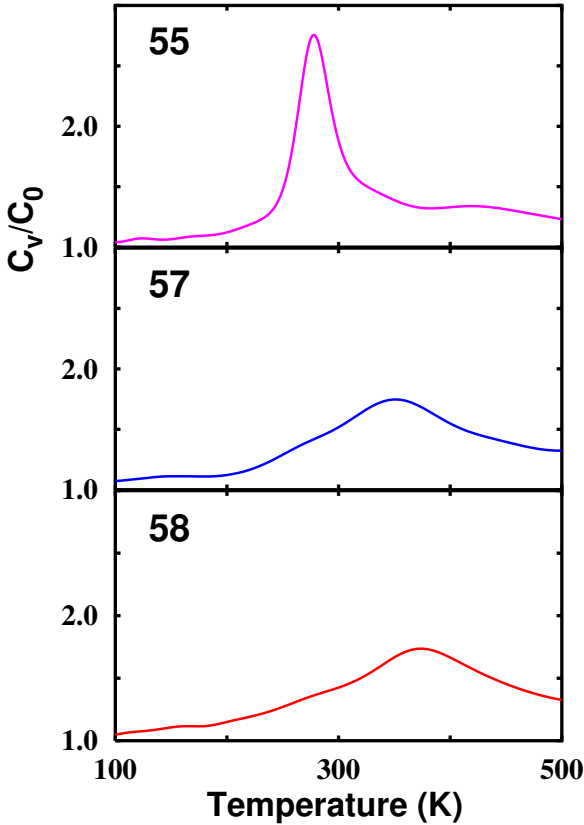


FIG. 7: The normalized specific heat as a function of temperature.  $C_0 = (3N - 9/2)k_B$  is the zero-temperature classical limit of the rotational plus vibrational canonical specific heat.

the nature of order or lack of order in the GS geometry and their finite temperature behavior, and between the connectivity of short bonds and its melting temperature. This explanation can be extended to the finite temperature behavior in Na<sub>50</sub> (figure not shown). Na<sub>50</sub> has a disordered GS geometry but does not possess a strongly connected network.<sup>11</sup> The specific-heat curve of Na<sub>50</sub>, indeed, shows a very broad melting transition with low melting temperature (225 K). The results of the density-functional simulations carried by Rytkönen *et al.*<sup>12</sup> as well as Lee *et al.*<sup>11</sup> are also consistent with the features that emerge out of our present calculation. An electronically closed-shell system Na<sub>40</sub> has a disturbed spherical GS geometry with a well-connected network of short bonds from core to surface atoms, which is stronger than that of Na<sub>55</sub>. Its specific heat is broader but melting point is higher than that of Na<sub>55</sub> (figure not shown). Thus, it also brings out the size-sensitive nature of specific heat curve in sodium clusters, not reported so far either experimentally or computationally. It may be noted that extreme size sensitivity of this kind has been observed experimentally in Ga and Al clusters.<sup>4</sup> We have also calculated the latent heats per atom by using caloric curves. They are estimated as 0.02 eV/atom for Na<sub>58</sub>, 0.016 eV for Na<sub>57</sub>, and 0.014 eV/atom for Na<sub>55</sub>. The latent heats observed by experiment<sup>1</sup> are 0.008 eV/atom

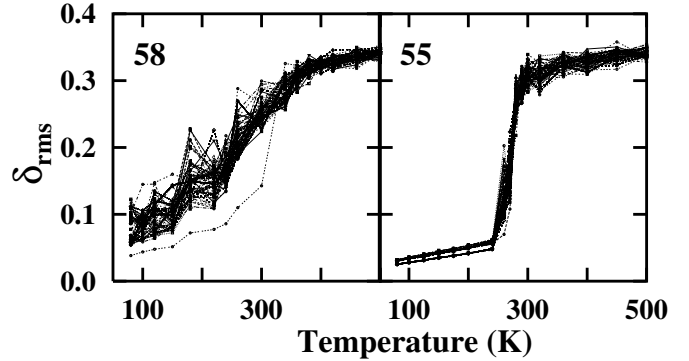


FIG. 8: The comparison of the root-mean-square bond length fluctuation ( $\delta_{rms}$ ) of individual atoms for Na<sub>58</sub> and Na<sub>55</sub>.

for Na<sub>57</sub> and 0.015 eV/atom for Na<sub>55</sub>. The deviation observed in Na<sub>57</sub> may be due to its very broad melting transition.

Due to the disordered nature of the GS geometry in Na<sub>58</sub>, we expect different atoms to move with various amplitudes at a given temperature. To see this, we have calculated the Lindemann criteria, i.e., the root-mean-square bond length fluctuation ( $\delta_{rms}$ ) for individual atoms of Na<sub>58</sub>, where  $\delta_{rms}(i)$  for atom *i* is defined as

$$\delta_{rms}(i) = \frac{1}{N} \sum_j \frac{\sqrt{\langle R_{ij}^2 \rangle_t - \langle R_{ij} \rangle_t^2}}{\langle R_{ij} \rangle_t}$$

where  $R_{ij}$  is the distance between *i* and *j* ions with  $i \neq j$ ,  $N = n - 1$  with  $n$  be number of atoms in the cluster, and  $\langle \dots \rangle_t$  denotes a time average over the entire trajectory. Indeed,  $\delta_{rms}(i)$  in Na<sub>58</sub> has a broad range of values at a given temperature showing a different response for each atom, while for Na<sub>55</sub> (highly symmetric structure) they are collective, leading to a sharp transition region. Further, it saturates at nearly 375 K in Na<sub>58</sub> compared to 280 K in Na<sub>55</sub>. Interestingly, the center atom in Na<sub>58</sub> (the bottom most line) dose not develop its melting behavior till 300 K. The disordered nature of the geometry leading to inhomogeneous distribution of bond strength results in distinctly different response of different atoms upon heating. We show the mean-square-displacement (MSD) of individual atoms at 240 K in Fig. 9. Evidently the atoms in these two clusters respond differently when heated. While Na<sub>55</sub> shows a clear solid-like behavior, a significant number of atoms in Na<sub>58</sub> show diffusive motion. We also observed the similar characteristics in Na<sub>57</sub>, seen in  $\delta_{rms}$  and MSD of Na<sub>58</sub>.

As shown in Fig. 10 where we calculate the average eigenvalues carried over the entire simulation runs of Na<sub>58</sub>, Na<sub>57</sub>, and Na<sub>55</sub>, we do not find that liquid-like and solid-like behavior of these clusters are electronically similar. Instead, the HOMO-LUMO gaps in all the cases are closed. According to the calculations of  $\varepsilon_{def}$  as a function of temperature, after melting their geome-

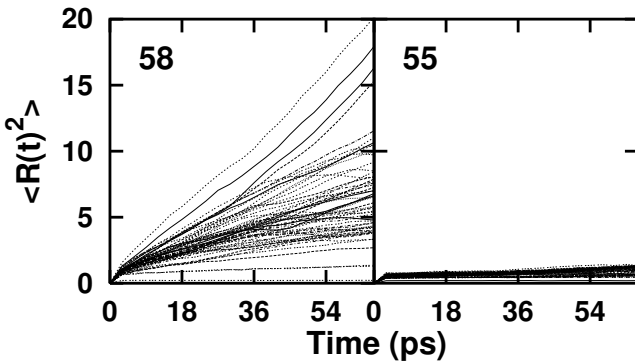


FIG. 9: The comparison of the mean square displacement (MSD) of individual atoms at 240 K for  $\text{Na}_{58}$  and  $\text{Na}_{55}$ .

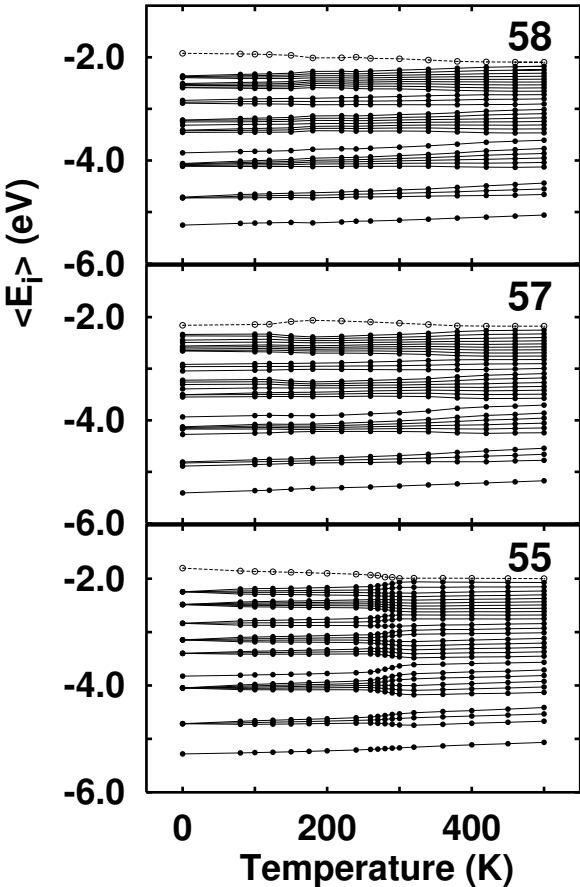


FIG. 10: The average eigenvalues of  $\text{Na}_{55}$ ,  $\text{Na}_{57}$ , and  $\text{Na}_{58}$  as a function of temperature.

tries become elongated in these clusters. This can explain the close of HOMO-LUMO gap. Thus, the present extensive simulations clearly bring out the importance and significance of the electronic structure. Interestingly, the change of eigenvalue spectrum and  $\varepsilon_{\text{def}}$  as a function of temperature in  $\text{Na}_{58}$  and  $\text{Na}_{57}$  becomes similar after 180 K. Even though the GS geometry of  $\text{Na}_{57}$  is not spherical, its structure changes towards spherical shape upon heating. Thus, when a cluster has both character-

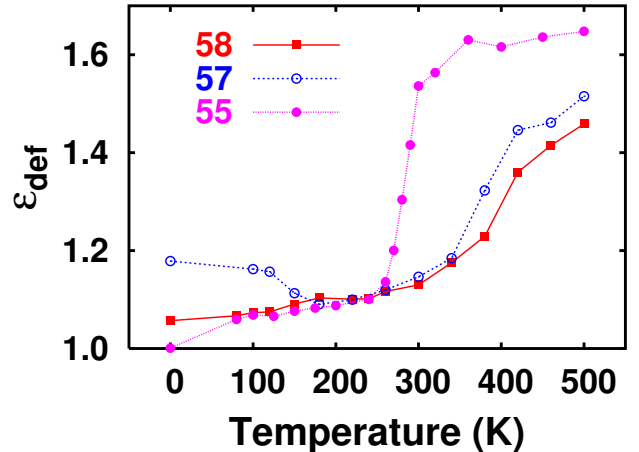


FIG. 11: The average deformation parameter of  $\text{Na}_{55}$ ,  $\text{Na}_{57}$ , and  $\text{Na}_{58}$  as a function of temperature.

istics of (nearly) closed shell not only geometrically but also electronically, it has high melting temperature compared to those having either geometric close shell or electronic closed shell. This may explain the reason  $\text{Na}_{142}$  has high melting temperature than  $\text{Na}_{138}$ , an electronic closed-shell cluster and  $\text{Na}_{147}$ , a geometric closed-shell one.

#### IV. SUMMARY

To summarize, the present work brings out the effect of the electronic as well as the geometric structures on the melting of  $\text{Na}_{58}$  and  $\text{Na}_{57}$  clusters compared with that of  $\text{Na}_{55}$ . The electronic shell-closing nature of  $\text{Na}_{58}$  drives the GS geometry to be spherical, which leads to a compact and disordered structure. As consequence, in  $\text{Na}_{58}$  the first-shell and surface as well as atoms on the surface are well connected with short bonds. This leads to the high melting temperature of nearly bulk melting temperature. The disordered nature of system is responsible for rather broad specific heat curve. Another example of strong connectivity is seen in the GS geometry of  $\text{Na}_{57}$ , nearly electronic shell closed cluster, which also shows high melting temperature than geometrically closed shell system of  $\text{Na}_{55}$ . The strong correlation between connectivity of bonds and melting temperature is also seen in the case of  $\text{Ga}^{13}$  and  $\text{Al}$  clusters.<sup>14</sup> Thus, we conclude that electronic structure affect its melting behavior strongly. We believe that it is possible to verify the prediction of present work experimentally with the calorimetry method.

#### V. ACKNOWLEDGMENTS

We acknowledge partial assistance from the Indo-French Center for Promotion for Advance Research (IFC-

PAR). We would like to thank Kavita Joshi and Sailaja Krishnamurty for a number of useful discussions.

---

<sup>\*</sup> Electronic address: mslee@unipune.ernet.in

<sup>†</sup> Electronic address: kanhere@unipune.ernet.in

<sup>1</sup> M. Schmidt, R. Kusche, B. von Issendorff, and H. Haberland, *Nature (London)* **393**, 238 (1998); R. Kusche, Th. Hippler, B. von Issendorff, and H. Haberland, *Eur. Phys. J. D* **9**, 1 (1999).

<sup>2</sup> M. Schmidt and H. Haberland, *C.R. Physique* **3**, 327, (2002); H. Haberland, T. Hippler, J. Donges, O. Kostko, M. Schmidt and B. von Issendorff, *Phys. Rev. Lett.* **94**, 035701 (2005).

<sup>3</sup> A. Aguado, J.M. López, *Phys. Rev. Lett.* **94**, 233401 (2005).

<sup>4</sup> G.A. Breaux, D.A. Hillman, C.M. Neal, R.C. Benirschke, and M.F. Jarrold, *J. Am. Chem. Soc.* **126**, 8628 (2004); G. A. Breaux, C. M. Neal, B. Cao, and M. F. Jarrold, *Phys. Rev. Lett.* **94**, 173401 (2005).

<sup>13</sup> K. Joshi, S. Krishnamurty, and D.G. Kanhere, *Phys. Rev. Lett.* **96**, 135703 (2006); S. Krishnamurty, S. Chacko, D.G. Kanhere, G.A. Breaux, C.M. Neal, and M.F. Jarrold, *Phys. Rev. B* **73**, 045406 (2006).

<sup>6</sup> Vienna *Ab initio* Simulation Package (VASP), Technische Universität Wien, 1999

<sup>7</sup> S. Chacko, D.G. Kanhere, and S.A. Blundell, *Phys. Rev. B* **71**, 155407 (2005).

<sup>8</sup> A. Vichare, D. G. Kanhere, and S. A. Blundell, *Phys. Rev. B* **64**, 045408 (2001); S. Krishnamurty, K. Joshi, D.G. Kanhere, and S.A. Blundell, *Phys. Rev. B* **73**, 045419 (2006).

<sup>9</sup> G. Wrigge, M. A. Hoffmann, and B. von Issendorff, *Phys. Rev. A* **65**, 063201 (2002).

<sup>10</sup> B. Silvi, and A. Savin, *Nature (London)*, **371**, 683 (1994).

<sup>11</sup> M.-S. Lee, S. Chacko, and D. G. Kanhere, *J. Chem. Phys.* **123**, 164310 (2005).

<sup>12</sup> A. Rytönen, H. Häkkinen, and M. Manninen, *Phys. Rev. Lett.* **80**, 3940 (1998).

<sup>13</sup> S. Krishnamurty, K. Joshi, S. Zorriasatein, and D. G. Kanhere, <http://arxiv.org/pdf/cond-mat/0608414>.

<sup>14</sup> to be published.